Exome-wide analysis implicates rare protein-altering variants in human handedness

Dick Schijven[1], Sourena Soheili-Nezhad[1], Simon E. Fisher[1,2], Clyde Francks[1,2,3]

[1] Language & Genetics Department, Max Planck Institute for Psycholinguistics, Nijmegen, The Netherlands; [2] Donders Institute for Brain, Cognition and Behaviour, Radboud University, Nijmegen, The Netherlands; [3] Department of Human Genetics, Radboud University Medical Center, Nijmegen, The Netherlands

Abstract

Handedness is a manifestation of brain hemispheric specialization. Left-handedness occurs at increased rates in neurodevelopmental disorders. Genome-wide association studies have identified common genetic effects on handedness or brain asymmetry, which mostly involve variants outside protein-coding regions and may affect gene expression. Implicated genes include several that encode tubulins (microtubule components) or microtubule-associated proteins. Here we examined whether left-handedness is also influenced by rare coding variants (frequencies ≤ 1%), using exome data from 38,043 left-handed and 313,271 right-handed individuals (UK Biobank). The beta-tubulin gene *TUBB4B* showed exome-wide significant association, with a rate of rare coding variants 2.7 times higher in left-handers (0.076%) than right-handers (0.028%). The *TUBB4B* variants were mostly heterozygous missense changes, but included two frameshifts found only in left-handers. Other *TUBB4B* variants have been linked to sensorineural and/or ciliopathic disorders, but not the variants found here. Among genes previously implicated in autism or schizophrenia by exome screening, *DSCAM* and *FOXP1* showed evidence for rare coding variant association with left-handedness. The exome-wide heritability of left-handedness due to rare coding variants was 0.91%. This study revealed a role for rare, protein-altering variants in left-handedness, providing further evidence for the involvement of microtubules and disorder-relevant genes.

Introduction

Roughly 90% of the human population is right-handed and 10% left-handed (1, 2). Despite some regional and temporal variation, this overall bias is broadly consistent across continents, and has been stable through human history (2-6). Handedness is a manifestation of brain asymmetry, as right handedness reflects left-hemisphere dominance for control of the preferred hand, and vice versa (7).

Population-level asymmetries of anatomy and function arise in the human brain during fetal development (8-13), and right-lateralized predominance of arm movements has been reported already at ten weeks of gestational age (14). The early appearance of these asymmetries indicates a genetically regulated program of left-right axis development in the central nervous system (1, 15-18). Consistent with this, left-handedness has shown heritability of roughly 25% in twin-based analysis (19), and 1-6% in population studies that have assessed the specific contribution of common genetic variants (20, 21). Twin- and family-based studies have also reported heritabilities of up to roughly 30% for measures of structural or functional brain asymmetry, particularly for regions or networks important for language (22-25), which is lateralized to the left hemisphere in most people.

Two large-scale genome-wide association studies of human handedness (20, 26) have been performed based on the UK Biobank adult population dataset (27), which included over 30,000 left-handed and 300,000 right-handed individuals. Three or four genomic loci showed statistically significant associations with left-handedness, depending on study-specific inclusion criteria and methods. The implicated genes included *TUBB* which encodes a beta-tubulin component of microtubules, and *MAP2* and *MAPT* which encode microtubule-associated proteins. Microtubules are prominent parts of the cytoskeleton – the framework of protein filaments internal to cells – that contributes to a wide range of processes including cellular growth, division, migration, shape and axis formation, axon outgrowth and intracellular transport (28). It is not known how microtubules affect inter-individual variation in human handedness, but it has been suggested (17, 29) that they may contribute to cellular

chirality early in brain development, and thereby to organ-intrinsic formation of the brain's left-right axis (see Discussion).

An even larger genome-wide association meta-analysis study of human handedness has also been performed, including the UK Biobank in addition to many other datasets, for a total of 194,198 left-handed and 1,534,836 right-handed individuals (21). The greater statistical power of this study resulted in 41 genomic loci being significantly associated with left-handedness, including at least eight that implicated tubulins or microtubule-associated proteins, and other genes involved in axon development and neurogenesis (21).

In addition, genome-wide association scanning using brain imaging data from over 32,000 UK Biobank individuals found 27 independent genetic variants that were significantly associated with different aspects of structural brain asymmetry (17). Remarkably, almost half of these loci implicated genes that code for tubulins or microtubule-associated proteins (17). A further study (29) then mapped cerebral cortical structural asymmetry with respect to handedness in 3,062 left-handers and 28,802 right-handers from the UK Biobank, and found that 18 of the 41 handedness-associated genomic loci (21) were also associated with at least one regional cortical asymmetry that is linked to left-handedness. The implicated genes again included several that encode tubulins: TUBB, TUBA1A/TUBA1B/TUBA1C (the latter three genes are clustered together in the genome), TUBB3 and TUBB4A, as well as microtubule-associated proteins MAP2, MAPT and NME7.

All of the large-scale studies mentioned above were based only on common genetic variation, i.e. with allele frequencies in the population of at least half of one percent. It is possible that rare, protein-altering variants also contribute to left-handedness, with larger effects on carriers than the common variants studied so far (30). One study in an extended, consanguineous family with numerous left-handers did not identify such effects using exome sequencing (31). In addition, an exploratory study of right-hemisphere language dominance – a trait with roughly 1% frequency that occurs mostly in left-handers – found tentative evidence for rare genetic contributions that implicated the actin cytoskeleton (32), but that study was based on fewer than 100 unrelated participants. Therefore, rare coding variation has yet to be explored in large-scale studies of human handedness. Identifying rare, coding effects on left-handedness may help to elucidate mechanisms of left-right axis development in the human brain.

Meta-analyses have indicated that left-handedness occurs at increased rates in neurodevelopmental disorders, including autism (33) and schizophrenia (34). In addition, large-scale studies have found that various aspects of structural brain asymmetry are subtly altered in autism (35) and schizophrenia (36). These associations suggest that population-typical asymmetries are linked to neurotypical function. Both autism and schizophrenia have shown genetic overlaps with structural brain asymmetry, in terms of common variant effects (17, 37). Rare, coding variants are also known to be involved in the genetic architecture of neurodevelopmental disorders (38, 39). While most left-handers do not have these disorders, the increased rates of left-handedness in these disorders suggests a minority of left-handedness might arise from rare, protein-coding variants.

Here we made use of exome sequence data from the UK Biobank to investigate the contribution of rare, coding variants to left-handedness. We used gene-based analysis to scan for individual genes associated with left-handedness, as well as burden heritability regression (40) to estimate the total, exome-wide contribution of this class of genetic variation.

Results

Exome-wide association scan for left-handedness

After sample-level quality control (Methods) there were 313,271 right-handed and 38,043 left-handed individuals (supplementary table 1). The rate of left-handedness can vary from roughly 2% to 14% in different regions of the world, which is thought primarily to reflect enforced right-hand use in some cultures (3, 5, 6, 41). To avoid confounding our genetic association analysis, we defined four separate, genetically homogeneous groups of UK Biobank individuals that correspond to major world

ancestries, using a combination of self-reported ethnicity and data-driven genetic clustering: Asian ancestry, Black ancestry, Chinese ancestry, and White ancestry (see Methods and Supplementary Figure 1). As expected, the rate of left-handedness varied between these clusters (Table 1). Within each cluster separately we would then test the association of genetic variants with handedness, and finally meta-analyze across clusters.

Ancestry cluster	Right-handed	Left-handed	Both hands equally	Total
Asian	6,421 (91.1%)	433 (6.1%)	198 (2.8%)	7,052
Black	5,237 (91.4%)	381 (6.7%)	111 (1.9%)	5,729
Chinese	1,178 (93.3%)	52 (4.1%)	33 (2.6%)	1,263
White	300,435 (87.4%)	37,177 (10.8%)	6,169 (1.8%)	343,781

Table 1. The numbers of individuals in each genetically-informed ancestry cluster, separately by self-reported handedness. Percentages are given within ancestry clusters.

There were also 6,511 individuals who reported using both hands equally (Table 1), but this trait was previously found to have poor repeatability in UK Biobank individuals who reported their handedness on more than one occasion (1). We excluded this group from our genetic association and heritability analyses.
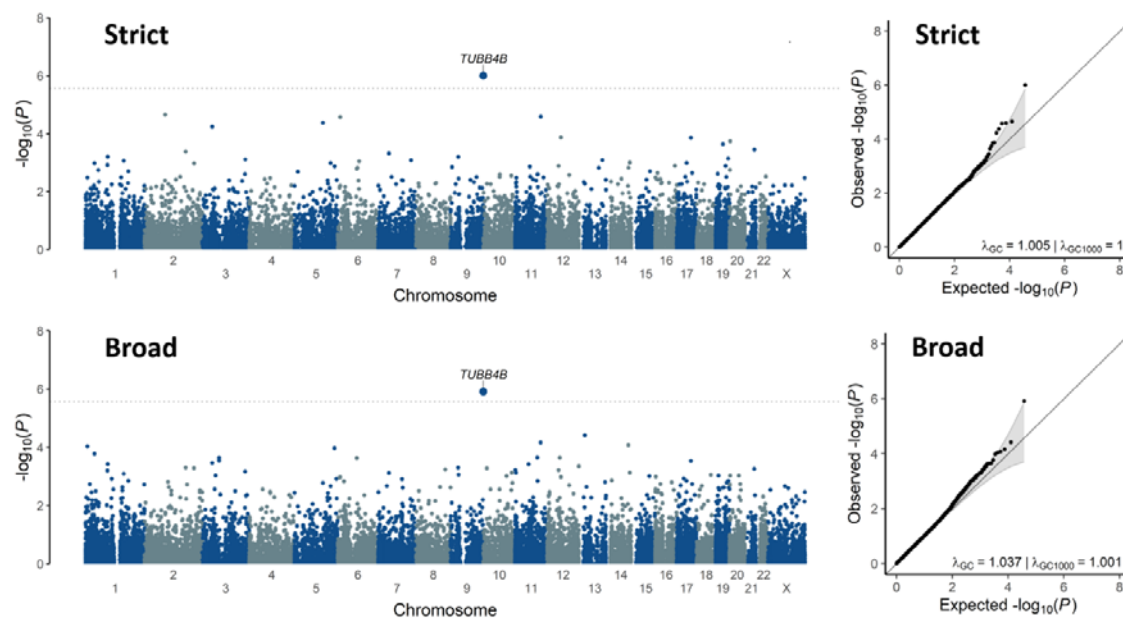
We focused on exonic variants with frequencies $\leq$ 1% that met sequence quality criteria (supplementary table 2, supplementary figure 2) and had high likelihoods of affecting protein function (Methods; supplementary table 3). This 'strict' set of variants included frameshift and stop mutations that affect canonical gene transcripts outside of the 5% tail ends of the corresponding proteins, and missense variants when they had Combined Annotation Dependent Depletion (CADD) phred-scaled scores > 20. CADD scores indicate the deleteriousness of genetic variants based on diverse genomic features derived from surrounding sequence context, gene model annotations, evolutionary constraint, epigenetic marks and functional predictions (42). We also defined a more inclusive, 'broad' set of variants that included all 'strict' variants plus other variants predicted to have less substantial effects on protein function (for missense variants this meant CADD phred scores > 1), again with frequencies $\leq$ 1% (see Methods; Supplementary Table 3).

Separately for the strict and broad variant sets, we ran gene-based association analysis with handedness (left-handed versus right-handed) using an additive burden framework, where each individual's number of minor alleles in a given gene was summed to compute a burden score for that individual and gene (43). Summary statistics were then meta-analyzed per gene across ancestry groups. There were 18,381 genes for the strict variant set and 18,925 genes for the broad variant set. Q-Q plots indicated appropriate control of type 1 error (Figure 1).

For both the strict and broad set of variants, one gene showed statistically significant association with handedness after multiple testing correction (Methods): the gene encoding microtubule component beta-tubulin TUBB4B, with association beta=1.07, P=9.9x10^{-7} for the strict set, and beta=1.06, P=1.2x10^{-6} for the broad set (Figure 1, Supplementary Figure 3). Other genes that showed suggestive evidence for association (with nominal association P values < 1x10^{-5}) for the strict and broad sets are shown in Supplementary Table 4. These included the gene that encodes TRAK1, involved in mitochondrial trafficking within axons and associated with neurodevelopmental delay and seizures (44), and myotubularin phosphatase MTMR6, involved in secretion and autophagy (45). The full exome-wide, gene-based meta-analysis results will accompany this paper as Dataset 1.

For each of 48 genes implicated in left-handedness by the largest previous genome-wide association study based on common genetic variants (21), we queried our exonic rare-variant association results from the present study. None of these genes showed significant rare-variant associations after Bonferroni correction for 48 tests, for either the strict or broad variant sets (Supplementary Table 5). The most significant individual result among these 48 genes was for *FOXN1* and the strict variant set, with beta=0.33, P=0.0067 (un-corrected). This gene encodes a transcription factor involved in

cutaneous and thymic epithelial cell development, but also embryonic central nervous system development (recessive mutation can cause anencephaly and spina bifida) (46).

Figure 1. Exome-wide, gene-based association testing in 38,043 left-handed and 313,271 right-handed individuals, based on rare protein-altering variants. Top: the strict variant set. Bottom: the broad variant set (that also included the strict variants for this analysis). Left: Manhattan plots show the genome along the x-axis and the gene-wise association significance levels on the y-axis. Dashed lines indicate Bonferroni-based multiple testing correction thresholds. Right: Q-Q plots corresponding to the Manhattan plots.
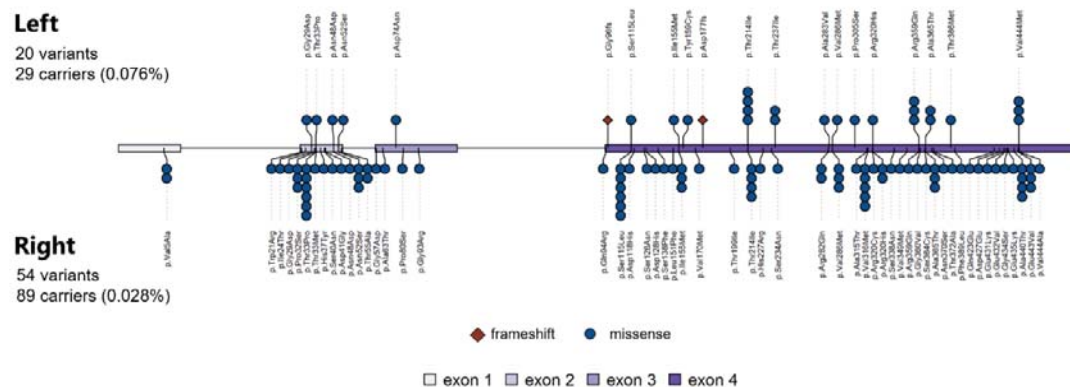
Rare TUBB4B variants in the general population

For *TUBB4B*, the strict variant set comprised 20 variants in 29 left-handed carriers, and 53 variants in 89 right-handed carriers (Figure 2). As left-handers comprised 10.8% of the individuals tested, their rate of rare, deleterious *TUBB4B* variants (0.076%) was 2.7 times higher than in right-handers (0.028%). All *TUBB4B* variants were heterozygous, and only one individual carried two different variants, such that many of the variants were present uniquely in single individuals (Figure 2). Only one *TUBB4B* variant was additionally included in the broad set that was not already included in the strict set (causing amino acid change Asp427Glu), which explains the similarity of strict and broad results for this particular gene. The *TUBB4B* association with left-handedness was therefore driven by variants that are strongly predicted to be disruptive and deleterious. Strict and broad results were sometimes more divergent for other genes (Figure 1; Supplementary Table 4; Dataset 1).

Most of the *TUBB4B* variants caused missense changes, i.e. substituting one amino acid for another at a given point in the protein sequence (Figure 2, Supplementary Figure 4; Supplementary Figure 5). However, there were two frameshift variants in left-handers, and none in right-handers (Figure 2), despite right-handers out-numbering left-handers by roughly 8:1. Frameshift variants disrupt the triplet reading frame of DNA and result in mis-translation of protein sequence from that point onwards. As such, they are among the most disruptive types of coding variant. Both of the frameshift variants that we found were predicted to cause degradation of the *TUBB4B* RNA transcript by nonsense-mediated decay (Methods). Therefore, both frameshift variants are likely to lead to haploinsufficiency.

Human TUBB4B shows extremely high conservation of amino acid identities with its orthologs in other vertebrates: 100% homology in chimpanzees, macaques, mice, cattle and dogs, 99.8% in rats, 99.6% in chickens, and 99.3% in clawed frogs (Methods). This high degree of conservation likely contributed to CADD predictions of deleteriousness for many of the *TUBB4B* missense variants, as

the gene appears largely intolerant to variation across vertebrates. As regards other, paralogous beta-tubulin genes, humans have eight of these: *TUBB*, *TUBB1*, *TUBB2A*, *TUBB2B*, *TUBB3*, *TUBB4A*, *TUBB6* and *TUBB8*. For each 'strict' variant in *TUBB4B* we assessed whether it alters the protein sequence at a site that varies between human beta-tubulin paralogs, or is fully conserved across these paralogs (Supplementary Figure 4). The two frameshift mutations were counted among those that affect conserved sites. 15 out of 29 left-handed carriers (52%) had variants that changed sites which are conserved across all paralogs, whereas 31 out of 89 right-handed carriers (35%) had such variants (Figure 2, Supplementary Figure 4). This suggests that TUBB4B variants observed in left-handers tend to affect especially critical sites, although the difference was not statistically significant (chi-square=2.62, one-tailed P=0.052).

Figure 2. Rare protein-altering TUBB4B variants found in left-handed individuals (top) and right-handed individuals (bottom). The number of individuals carrying a given variant is indicated by the number of symbols (circles or diamonds) for that variant. All variants were heterozygous, and only one individual carried two different variants. Exons and introns of the genomic locus are indicated in the central schema. All but one of the variants (Asp427Glu) met the 'strict' criteria for being deleterious. Frameshift mutations were only found in left-handers. Left-handers comprised 10.8% of the individuals in the analyzed dataset, but 32.6% of TUBB4B variant carriers.

Other rare, heterozygous *TUBB4B* missense variants, and also an in-frame ten amino acid duplication, are known to cause sensorineural and/or ciliopathic disorders which can involve infant blindness and early onset hearing loss (47-49) (see Discussion). However, none of the specific TUBB4B amino acid changes that we identified in the UK Biobank were reported in previous clinical genetic studies, and neither were any frameshift mutations. We tested whether TUBB4B variant carriers in the UK Biobank showed group-average differences from the rest of the dataset in terms of speech reception thresholds or visual acuity, or in the frequency of hearing problems, use of a hearing aid, eye problems or use of glasses, while controlling for age and sex (Methods). No associations were significant (all P values > 0.25), which indicates that hearing and vision are not generally affected by the *TUBB4B* coding variants found in the UK Biobank population dataset (Supplementary Table 6).

Gene-based burden heritability of left-handedness

To quantify the heritability of left-handedness attributable to the genome-wide burden of rare, exonic variants, we applied burden heritability regression (40) (Methods). This analysis was performed only in the genetically-informed 'White' ancestry cluster, as this was the only cluster with a sufficiently large number of individuals for this type of analysis (300,435 right-handed and 37,177 left-handed; Table 1). Variants were stratified by strict versus broad annotations (for this specific analysis the strict variants were removed from the broad set in order to distinguish the heritability arising from deleterious versus relatively benign variants). We also stratified into three variant frequency bins, i) minor allele frequency $<1 \times 10^{-5}$; ii) $1 \times 10^{-5} \leq$ minor allele frequency $<1 \times 10^{-3}$); iii) $1 \times 10^{-3} \leq$ minor allele frequency $\leq 1 \times 10^{-2}$.

Aggregated across the three frequency bins and strict and broad variants, the burden heritability best estimate (liability scale) was 0.91% (standard error 0.32%) (Table 2). For 'strict' variants the main contribution was from the two rarest frequency bins (minor allele frequencies $< 1 \times 10^{-3}$), whereas for

'broad' variants those with minor allele frequencies above 1×10^{-5} and up to 1% made the main contributions (Table 2). Removing *TUBB4B* from the analysis made little impact on the burden heritability estimates (Table 2), which confirms that the population-level, exome-wide burden heritability involves multiple additional loci beyond this single gene.

Functional group	Minor allele frequency (MAF)	All genes			TUBB4B excluded		
		Heritability	SE	Genes	Heritability	SE	Genes
Strict	MAF < 1×10^{-5}	0.14%	0.13%	16891	0.16%	0.13%	16890
Strict	$1 \times 10^{-5} \leq$ MAF < 1×10^{-3}	0.32%	0.14%	16584	0.29%	0.14%	16583
Strict	$1 \times 10^{-3} \leq$ MAF $\leq 1 \times 10^{-2}$	-0.04%	0.10%	6476	-0.04%	0.10%	6476
Strict	Aggregate	0.41%	0.24%	NA	0.41%	0.24%	-
Broad minus strict	MAF < 1×10^{-5}	0.08%	0.08%	16952	0.09%	0.08%	16951
Broad minus strict	$1 \times 10^{-5} \leq$ MAF < 1×10^{-3}	0.18%	0.10%	16508	0.18%	0.10%	16508
Broad minus strict	$1 \times 10^{-3} \leq$ MAF $\leq 1 \times 10^{-2}$	0.24%	0.12%	5787	0.24%	0.12%	5787
Broad minus strict	Aggregate	0.50%	0.17%	NA	0.51%	0.17%	-
All	Aggregate	0.91%	0.32%	NA	0.92%	0.32%	-

Table 2. Burden heritability regression for left-handedness shows the proportion of trait disposition due to rare, exonic variants considered over the whole genome. Liability-scale heritability estimates are presented separately by variant functional groups and frequency bins, as well as aggregated. For this specific analysis (unlike the gene-based exome-wide association scan), the strict variants were removed from the broad set, in order to distinguish the contributions to heritability from disruptive versus more subtle variants. Results are shown before and after excluding TUBB4B. SE: standard error of the heritability estimate. 'Genes' refers to the number of genes included in the analysis for a given variant frequency bin.

Rare coding variant associations with autism and schizophrenia in comparison to left-handedness

Recent large-scale association studies based on rare, coding variants identified 24 genes associated with autism (38) and 10 genes associated with schizophrenia (39) at exome-wide significance levels. We queried each of these 34 genes in the rare-variant association results of the present study of left-handedness (Supplementary Tables 7 & 8). The autism-associated gene *DSCAM* (Down syndrome cell adhesion molecule) showed significant association with left-handedness after Bonferroni correction for 34 tests (strict set, beta=0.17, P=0.00036 uncorrected: broad set, beta=0.15, P=0.00055 uncorrected) (Supplementary Table 7). *DSCAM* is involved in central and peripheral nervous system development, including through affecting the interaction of other autism-linked synaptic adhesion molecules (50). In addition, the autism-associated gene *FOXP1* showed significant association with left-handedness after Bonferroni correction for 34 tests for the broad set only (beta=0.17, P=0.00023 uncorrected) (Supplementary Table 7). *FOXP1* encodes a transcription factor in which disruptive coding variants are known to cause a developmental disorder that includes intellectual disability, autistic features, speech/language deficits, hypotonia and mild dysmorphic features (51).

Discussion

By making use of the large UK Biobank general population dataset for exome-wide screening and burden heritability analysis, our study identified a role for rare, coding variants in left-handedness. At the population level, the heritability of left-handedness due to this class of genetic variant was low, at just under 1%. Nonetheless, the carriers of rare coding variants in *TUBB4B,* and potentially also *DSCAM* and *FOXP1,* appear to have substantially higher chances of being left-handed than non-carriers. Implicating these specific genes in left-handedness provides potential insights into mechanisms of left-right axis formation in the brain, as well as genetic susceptibility to brain disorders.

As mentioned in the Introduction, several other tubulin genes have been implicated in both left-handedness and structural brain asymmetry by large-scale studies of common genetic variation, including *TUBB*, the *TUBA1A/TUBA1B/TUBA1C* cluster on chromosome 12, *TUBB3* and *TUBB4A*, as well as microtubule-associated proteins *MAP2*, *MAPT* and *NME7* (17, 21, 29). It is therefore especially striking that in a systematic screen of rare coding variation across the entire exome, *TUBB4B* showed the most significant association with left-handedness in the present study. This finding gives further support for the involvement of microtubules in human brain asymmetry. While the common variants implicating tubulin genes are non-coding and likely to affect gene expression levels, the coding variants in *TUBB4B* indicate that protein sequence changes of this gene can affect handedness and brain asymmetry.

Other heterozygous missense variants in *TUBB4B* have been linked to sensorineural and/or ciliopathic disorders (47-49), but not the specific coding variants that we found in the UK Biobank. Our findings therefore extend the spectrum of phenotypes associated with rare coding *TUBB4B* variants to include the benign trait of left-handedness. It is thought that some of the heterozygous *TUBB4B* missense variants that cause disorders act in a dominant-negative manner, through altering microtubule stability and dynamics which can affect microtubule growth (47-49). A dominant-negative effect arises when an altered protein adversely affects its normal, unaltered counterpart within the same heterozygous cell. It is possible that some of the heterozygous missense *TUBB4B* variants in the UK Biobank exert dominant-negative effects that impact microtubule dynamics, but less substantially than the variants that have been linked to clinical disorders. Interactions with microtubule-associated proteins may also be affected. In addition, the two frameshift-causing variants that we found in left-handers in the UK Biobank suggest that haploinsufficiency of *TUBB4B* might affect brain asymmetry, but again without a clinical phenotype.

One of the many cellular functions of microtubules is in motile cilia, which are organelles that project from the cellular surface and can beat/rotate to produce an extracellular fluid flow (52). Life on earth is based on L-form amino acids rather than the mirror D-form, and this chirality carries through to the macromolecular scale to influence the structure and movement of cilia (52, 53), i.e. they tend to beat/rotate in one particular orientation rather than the other. In the early embryos of many mammalian species, this results in unilateral, leftward fluid flow that can trigger asymmetrical gene expression (52). Lateralized, downstream developmental programs eventually give rise to asymmetries of visceral organ placement and morphology (of the heart, lungs etc.).

Microtubules support the hair-like structure of cilia and contribute to their motility. Therefore, embryonic motile cilia might seem to provide a potentially common mechanism for the developments of brain and visceral asymmetry. However, the typical left-hemisphere dominances for hand preference and language do not usually reverse in people with *situs inversus* and primary ciliary dyskinesia, a rare genetic condition that involves reversal of the visceral organs on the left-right axis, together with impairment of motile ciliary function (54-57). Furthermore, mutations in tubulin genes are not known as causes of *situs inversus* of the viscera. Together, these observations suggest a developmental disconnect between brain and visceral asymmetries.

As components of the cytoskeleton, microtubules can also contribute to asymmetries at the whole-cell scale, i.e. create uni-directional biases in the morphology, position, rotation or migration of cells (58), or the intracellular distributions of organelles (59). In invertebrates and frog embryos, cellular chirality during embryonic development can induce asymmetrical morphology of certain organs, independently of other developing organs or systems (58, 60-66). Therefore, the cytoskeleton may be a source of left-right axis creation, in addition to motile cilia. An organ-intrinsic, microtubule-based, but non-motile-ciliary mechanism of brain left-right axis formation would fit the human genetic findings that have implicated tubulins such as *TUBB4B* in handedness, and also match with the disconnect between brain and visceral asymmetries (17). An involvement of non-motile cilia is also possible.

Brain magnetic resonance imaging (MRI) data was only available for 13 of the UK Biobank *TUBB4B* variant carriers (left- and right-handers together), which is too small a sample for reliable association mapping with respect to brain structural or functional asymmetries. Neither of the left-handed

frameshift variant carriers had MRI data. Studies that identified other *TUBB4B* mutations in sensorineural and/or ciliopathic disorders also did not report brain scanning (47-49). However, mutations in different beta-tubulin genes in humans have been identified as causes of extremely rare neurological disorders (67), and some of those clinical genetic studies did include brain imaging data. Intriguingly, mutations in *TUBB2B* can cause asymmetrical polymicrogyria (many and small folds) of the cerebral cortex (68). Mutations in *TUBB3* can cause asymmetrical cortical dysplasia and unilateral hypohidrosis (reduced sweating on one side of the body, thought to be linked to disrupted function of the cortex, brain stem, and spine) (69, 70). It may therefore be informative to collect brain MRI data from *TUBB4B* variant carriers in future studies.

More generally, the spectrum of disorders attributable to mutations in alpha- and beta-tubulin isotypes includes features consistent with altered neuronal migration and differentiation, as well as axon guidance and maintenance (67). The present study suggests that brain left-right axis formation may be another aspect, although as microtubules are multi-functional and essential components of cells, they may also affect asymmetrical brain development through various downstream mechanisms. For instance, assembled microtubules have 'plus-ends' and 'negative-ends' with specialized functions that contribute to developmental processes such as directional migration of progenitor cells, and axonal/dendritic polarity (71)

As regards *DSCAM* and *FOXP1*, although these genes were not significantly associated with left-handedness in the context of exome-wide multiple testing, they showed evidence for association with left-handedness in a targeted look-up of 34 genes that were previously implicated in autism or schizophrenia at exome-wide significant levels, by large-scale studies (38, 39). Specifically, rare-coding variants in *DSCAM* and *FOXP1* were implicated in autism by a multi-cohort, exome-wide analysis that included nearly 12,000 affected individuals (38). The present study suggests that rare, coding variants in these genes are also relevant to left-handedness, which raises the possibility that altered development of the brain's left-right axis is part of the etiology of these disorders, when caused by *DSCAM* or *FOXP1* mutations.

Mutations or copy-number variants affecting *DSCAM* have also been associated with intellectual disability and schizophrenia, and this gene might additionally contribute to the phenotype of Down's syndrome (72, 73). *DSCAM* encodes a cell surface receptor and cell adhesion molecule. In the nervous system DSCAM affects various neurodevelopmental processes including neuronal migration, axon growth and branching, synapse development and synaptic plasticity (50, 73). In mice, DSCAM contributes to the formation of the spinal locomotor circuit, and is also important in voluntary locomotor control through affecting short-term plasticity and synaptic integration within the motor cortex (74). Such functions may be relevant to the possible association of *DSCAM* with handedness in humans. The transcription factor encoded by *FOXP1* is involved in a neurodevelopmental disorder that involves intellectual disability with autistic features, together with language impairment (51). The speech and language phenotype can include dysarthria, motor planning and programming deficits, and linguistic-based phonological errors (75). The latter aspects may be especially linked to altered brain asymmetry.

We found that the heritability of left-handedness that was attributable to rare, coding variants, when considered over the whole exome, was just under 1%. This compares to a common single-nucleotide polymorphism (SNP) based heritability for left-handedness of 1-6% in the UK Biobank (20, 21). For a further comparison, schizophrenia and bipolar disorder have shown liability-scale burden heritabilities of 1.7% and 1.8% respectively, when considering predicted loss-of-function variants specifically (40). Our finding of a significant exome-wide heritability for left-handedness suggests that more genes will be implicated in this trait by rare variant association mapping in even larger, future studies.

Twin studies have not found effects of shared family environment on brain asymmetries (22, 23), and left-handedness has shown limited associations with the environmental and early life factors that have been studied to date (1, 76). Most of the variation in brain and behavioural asymmetries may therefore arise stochastically in early development (77). The low burden heritability and SNP-based heritability of left-handedness, together with the strong population-level bias to right-handedness in the population, suggest that developmental mechanisms for brain asymmetry are largely genetically

invariant in the population. This may reflect negative selection of variants in genes involved in brain asymmetry (20, 78, 79). A microtubule-based mechanism of brain left-right axis formation would be consistent with this, because microtubules are essential for many other, fundamental cellular functions (80, 81). Accordingly, the TUBB4B protein shows over 99% conservation of amino acid sequence across many vertebrate species.

In conclusion, this study revealed a role for rare, protein-altering variants in human handedness, and provided further evidence that microtubules are involved – possibly through affecting molecular, organelle or cellular chirality early in development. This study also shed light on possible commonalities and differences between rare, coding contributions to left-handedness and brain-related disorders.

Materials and methods

Data set

For this study we used data from the UK Biobank (82, 83). The study was conducted as part of approved project 16066, with Clyde Francks as the principal investigator. The UK Biobank received ethical approval from the National Research Ethics Service Committee North West-Haydock (reference 11/NW/0382), and all of their procedures were performed in accordance with the World Medical Association guidelines (27). Written informed consent was provided by all of the enrolled participants. Some of our analyses were conducted on the UK Biobank research analysis platform (https://ukbiobank.dnanexus.com).

Phenotype data were obtained from data release version 10.1 (available on the research analysis platform since 14 April 2022), and the whole exome sequence data were from release version 12.1 (available on the platform since 29 June 2022). We selected 'Handedness (chirality/laterality)' (data-field 1707) as our primary phenotype, which was self-reported according to the question 'Are you right or left handed?' (presented on a touchscreen). Possible answers were 'right-handed', 'left-handed', 'use both left- and right hands equally' and 'prefer not to answer'. The latter was treated as missing data. Answers were recorded at a maximum of three visits to a UK Biobank assessment center. We used the handedness reported at the first non-missing instance. For individuals who had reported their hand preference at multiple instances, those who were inconsistent in their reported handedness were excluded.

For all individuals with stable handedness data, we selected additional variables to use as covariates: 'Sex' (data-field 31), 'Year of birth' (data-field 34), 'Country of birth' (UK versus elsewhere; data-field 1647), 'Part of a multiple birth' (data-field 1777), the first 40 principal components derived from common variant genotype data that capture population ancestry (data-field 22009), and the exome sequencing batch (i.e. a binary variable to indicate whether an individual was sequenced as part of the first 50,000 exome release or subsequent releases, due to a difference in the flow cells used). 'Country of birth' and 'Part of a multiple birth' could be recorded at multiple instances, and again we set these to missing if individuals reported inconsistent answers.

Defining ancestry clusters

We first grouped 469,804 individuals with exome data into five major ancestry subgroups according to self-reported ethnic identities in data-field 21000: Asian or Asian British, Black or Black British, Chinese, Mixed, and White. Answers of 'Do not know' or 'Prefer not to answer' were set to missing. Ethnicity was reported at up to four visits. Individuals were only assigned to an ancestry group if they had non-missing data for at least one instance, and consistently reported their ethnicity if reported at multiple instances. For each of the self-reported ethnic groups separately, we then applied a Bayesian clustering algorithm in the R package, called 'aberrant', to genetic ancestry principal components 1-6 (from data-field 22009). This software seeks to define clusters of datapoints and any outliers from them (84). Individuals whose self-reported ethnicity was 'Other' were allowed to cluster with one of the Asian or Asian British, Black or Black British, Chinese, Mixed, or White groups, if they would fit according to their genetic data. The 'aberrant' package can only cluster along two dimensions, and

was therefore run separately three times for each self-reported ethnic grouping: first on principal components 1&2, then 3&4, then 5&6, with inlier threshold lambda=40. Individuals in the intersect of all three clusters for a given ethnicity were then assigned to one final genetically-informed cluster for each ethnic group. For the 'mixed' ancestry group we obtained a highly dispersed cluster, and therefore these individuals were excluded. See Table 1, supplementary figure 1 and supplementary table 1 for further information.

Sample-level filtering

There were initially 469,316 individuals with whole exome sequence data, handedness data, and who consistently reported their country of birth and whether they were part of a multiple birth. We then applied further individual-level quality control. First, individuals with missing data for one or more covariates defined above were excluded. Then we excluded individuals with discordant self-reported and genetically determined sex, as well as those not included in one of the genetically-informed ancestry clusters as described above. For pairs of related individuals inferred as third-degree relatives or closer (kinship coefficient > 0.0442) based on common variant data (84), we excluded one individual from each pair, prioritizing the removal of right-handed individuals and those present in multiple pairs, but otherwise randomly.

In total, 138,491 individuals were removed by all of these steps together (see Supplementary Table 1 for details), leaving 357,825 individuals. Of these, 313,271 were right-handed, 38,043 were left-handed, and 6,511 reported using both hands equally. See Table 1 for a breakdown by ancestry clusters. As mentioned earlier, the 'both hands equally' phenotype was not considered in our genetic association and heritability analyses due to a relatively low sample size and poor repeatability, but these individuals were included in our exome sequence pre-processing pipeline, described in the following section.

Whole exome sequence data and filtering

Whole-exome sequencing was performed by the UK Biobank according to protocols described elsewhere (85, 86)). Briefly, exomes were captured with the Integrated DNA Technologies xGen Exome Research Panel v1.0 including supplementary probes, targeting 39 megabase pairs of the human genome. Sequencing was performed on the Illumina NovaSeq 6000 platform and data were processed using the original quality functionally equivalent (OQFE) protocol (85): raw reads were mapped with the bwa-mem algorithm to the GRCh38 reference human genome, retaining all supplementary alignments. Duplicate reads were marked with Picard 2.21.2. Variants were called with DeepVariant 0.10.0 and restricted to exome capture regions plus the 100 base pairs flanking each capture target, resulting in a genomic variant-call file (gVCF) per sample. gVCFs were then merged using GLnexus 1.2.6 into multi-sample project-level VCF (pVCF) files.

We successively applied genotype- and variant-level filters to the exome data of the 357,825 individuals that remained after sample-level filtering in the pVCF files (86, 87). First, we only kept variants in the exome sequence target regions (as defined in UK Biobank resource 3803), excluding variants in the 100 base pair flanking regions for which reads had not been checked for coverage and quality metrics in the exome processing pipeline. We also removed any monoallelic variants that arose during merging of the individual-level VCFs. Then, we set individual-level genotypes to no-call if the read depth was < 7 for single-nucleotide variant sites or < 10 for insertion-deletion sites, and/or if the genotype quality score (GQ) was < 20. Variant-level filtering comprised removal of variant sites with an average GQ across genotypes < 35, variant missingness rate > 0.10, minor allele count < 1, and/or allele balance for variants with exclusively heterozygous genotype carriers < 0.15 for single-nucleotide variants and < 0.20 for insertion-deletions. Transition-transversion ratios were calculated prior to, and after, variant-level filtering. Filtered pVCF files were converted to PLINK-format binary files, excluding multi-allelic variants, and then merged per chromosome. For chromosome X, pseudo-autosomal (PAR) regions (PAR1: start - basepair 2781479, PAR2: basepair 155701383 – end) were split off from the rest of chromosome X. Any heterozygous genotypes in the non-PAR chromosome X in males were set to missing. See Supplementary Table 2 for the numbers of variants removed at each quality-control filtering step, and Supplementary Figure 2 for the distribution of numbers of variants per gene after these filters.

Functional annotation and masks

Functional annotation of variants in pVCF files was performed using snpEff v5.1d (build 2022-04-19) (88). Variants were assigned to genes based on their physical positions in the genome, and were assigned descriptive annotations using information derived from the Ensembl database (release 105). Additionally, variants were annotated with Combined Annotation Dependent Depletion (CADD) Phred scores from the database for nonsynonymous functional prediction (dbNSFP) (version 4.3a) (89) using the snpEff toolbox snpSift 5.1d (build 2022-04-19).

We then classified variants for downstream analyses based on their functional annotations. We first defined a 'strict' set of variants with the highest confidence for altering protein function and being deleterious. Strict variants had a 'High' annotation for affecting a canonical gene transcript outside of the 5% tail end of the corresponding protein (variants of this type include highly disruptive mutations such as frameshifts), or else a 'Moderate' annotation for affecting a canonical transcript together with a CADD Phred score of at least 20 (variants of this type are typically protein-altering missense variants that are especially likely to be deleterious) (Supplementary Table 3).

We then defined a more inclusive, 'broad' set of variants that included all of the strict variants in addition to several other categories with more equivocal evidence for altering protein function: 'High' annotated variants that affected alternative gene transcripts outside of 5% tail ends, 'Moderate' annotated variants that affected canonical or alternative gene transcripts with CADD Phred scores of at least 1, and 'Modifier' variants that affected canonical or alternative gene transcripts with CADD Phred scores of at least 1 (Supplementary Table 3).

Gene-based association analysis

We applied gene-based association testing using the regenie software (43), which broadly consists of two steps. First, to fit a whole genome regression model to capture phenotypic variance attributable to common genetic effects, we selected a high-quality subset of genetic markers from UK Biobank genotype array data (data category 263). Single-nucleotide polymorphisms with minor allele frequency $\geq$ 1%, Hardy-Weinberg Equilibrium test p-value > 1 x 10^{-15} (not for non-PAR chr X), and genotype missingness rate $\leq$ 1% were selected. We removed variants with high inter-chromosomal linkage disequilibrium according to Mbatchou *et al.* (43) and further pruned the data to remove intra-chromosomal linkage disequilibrium (r^2 threshold of 0.9 with a window size of 1000 single-nucleotide polymorphisms and a step size of 100 single-nucleotide polymorphisms), leaving 502,765 single-nucleotide polymorphisms for whole-genome model fitting and calculation of leave-one-chromosome-out (LOCO) predictions.

LOCO predictions were used as input in step 2, together with filtered exome data, handedness phenotypes and covariates as defined above. We ran gene-based analysis with the '*sum*' burden function, with alternative allele frequency threshold of $\leq$ 1%, and run separately for our strict and broad variant annotation masks (where broad included all strict variants too). Firth likelihood ratio testing was applied in regenie to correct gene p-values < 0.05 for the unbalanced left:right handed ratio of the study sample. Genes were tested when at least one variant mapped to a given gene. We then meta-analyzed burden association statistics separately for each gene across the four ancestry groups, using inverse-variance weighted meta-analysis in the METAL software (90). Finally, we applied a Bonferroni-adjusted significance threshold of 2.7 x 10^{-6} to account for testing of 18,381 genes with the strict mask, and 2.6 x 10^{-6} for testing 18,925 genes with the broad mask.

Burden heritability regression for left-handedness

Burden heritability can be estimated by regressing gene burden trait-association statistics on gene burden scores, where the heritability estimate is proportional to the regression slope, while population stratification and any residual relatedness affect the intercept (40). As left- and right-handedness are categorical traits in the UK Biobank data, for each autosomal variant we first obtained the allele counts (40) with respect to left- versus right-handedness, output from per-variant association analysis in regenie (under an additive model) (43). We then estimated burden heritability using the BHR package (40), stratified by three allele frequency bins: i) minor allele frequency < 1 x 10^{-5}; ii) 1 x 10^{-5} $\leq$ minor allele frequency < 1 x 10^{-3}); iii) 1 x 10^{-3} $\leq$ minor allele frequency $\leq$ 1 x 10^{-2}, and also stratified

by strict versus broad variant types (for this particular analysis the strict variants were removed from the broad set, unlike for the gene-based association scan described above, where the broad set included all strict variants too). We also used BHR to aggregate the burden heritability across frequency bins and across strict and broad variants. The observed-scale burden heritability estimate was converted to a liability-scale estimate, using a sample prevalence of 11% and a population prevalence of 10.4% for left-handedness (2).

TUBB4B analysis

For the *TUBB4B* gene we mapped all 62 variants with 'strict' functional annotations onto the canonical protein sequence (National Centre for Biotechnology Information reference NP_006079), and also with respect to each of the eight other human beta-tubulin paralogous proteins: TUBB (UQL51120), TUBB1 (NP_110400), TUBB2A (NP_001060.1), TUBB2B (NP_821080), TUBB3 (NP_006077), TUBB4A (NP_001276058), TUBB6 (AAI11375), TUBB8 (NP_817124) (Supplementary Figure 4). Some variants were present in more than one individual (Figure 2). We counted how many left-handed and right-handed individuals carried variants that altered variable sites as opposed to conserved sites in the various human beta-tubulin paralogs. The two *TUBB4B* frameshift variants were counted among those that affect conserved sites.

For the two frameshift variants, we also used NMDEscPredictor (91) to predict whether they are subject to degradation by nonsense-mediated decay, through introducing premature stop codons. The frameshift variants were: position 360, -1 and position 604, -4 according to RefSeq transcript NM_006088.

For cross-species comparisons, sequence alignment of human TUBB4B protein (NP_006079.1) was measured against its orthologs in *Pan troglodytes* (NP_006079.1)*, Macaca mulatta* (NP_006079.1)*, Mus musculus* (NP_006079.1)*, Rattus norvegicus* (NP_006079.1), *Bos taurus* (NP_006079.1)*, Canis lupus familiaris* (NP_006079.1)*, Gallus gallus* (NP_006079.1) and *Xenopus tropicalis* (NP_006079.1), using blastp (https://blast.ncbi.nlm.nih.gov/Blast.cgi?PAGE=Proteins).

We visualized the locations of the 60 'strict' missense changes with respect to the three dimensional structure of the human TUBB4B protein, using MutationExplorer (92) (supplementary figure 5). For this we input Protein Data Bank model 'AF-P68371-F1-model_v4' of the human TUBB4B protein, as generated by AlphaFold (93).

We tested whether TUBB4B variant carriers showed group differences compared to the rest of the UK Biobank individuals for several continuous or categorical traits related to vision and hearing: Speech Reception Threshold, i.e. the signal-to-noise ratio at which half of presented speech could be understood correctly (UK Biobank fields 22219 (left ear) and 20021 (right ear)); Visual acuity (fields 5187 (left eye) and 5185 (right eye)); Hearing difficulties/problems (field 2247); Hearing aid user (field 3393); Eye problems/disorders (field 6148); Wears glasses or contact lenses (2207). These tests were performed using general linear modelling for continuous traits and binomial regression for categorical traits, controlling for age and sex (Supplementary Table 6).

Disclosures

The authors declare no competing interests.

Acknowledgements

Data and Materials Availability

The primary data used in this study are from the UK Biobank. These data can be provided by UK Biobank pending scientific review and a completed material transfer agreement. Requests for the data should be submitted to the UK Biobank: www.ukbiobank.ac.uk. Specific UK Biobank data field codes are given in the Methods section. Some of our analyses were conducted on the UK Biobank research analysis platform (https://ukbiobank.dnanexus.com), as individual-level exome data cannot be downloaded from the latest release.

The openly available data sources and software used in this study are cited in the Methods section. Our meta-analyzed gene-based association summary statistics will accompany this paper as Dataset 1.

Author Contributions

Conceptualization: DS, SEF, CF. Data curation: DS, SSN. Formal analysis: DS. Funding acquisition: CF, SEF. Investigation: DS, CF. Methodology: DS, SSN, CF. Project administration: CF. Resources: CF, SEF. Software: DS. Supervision: CF. Visualization: DS, CF. Writing - original draft: DS, CF. Writing - review & editing: DS, SSN, SEF, CF.

References

1.   de Kovel CGF, Carrión-Castillo A, Francks C. A large-scale population study of early life factors influencing left-handedness. Scientific reports. 2019;9(1):584.
2.   Papadatou-Pastou M, Ntolka E, Schmitz J, Martin M, Munafò MR, Ocklenburg S, et al. Human handedness: A meta-analysis. Psychological bulletin. 2020;146(6):481-524.
3.   Coren S, Porac C. Fifty centuries of right-handedness: the historical record. Science. 1977;198(4317):631-2.
4.   Faurie C, Raymond M. Handedness frequency over more than ten thousand years. Proceedings of the Royal Society of London Series B: Biological Sciences. 2004;271(Suppl 3):S43-S5.
5.   McManus IC. The history and geography of human handedness. In: Sommer IEC, Kahn RS, editors. Language Lateralization and Psychosis. Cambridge: Cambridge University Press; 2009. p. 37-58.
6.   Perelle IB, Ehrman L. An international study of human handedness: the data. Behavior Genetics. 1994;24(3):217-27.
7.   Willems RM, der Haegen LV, Fisher SE, Francks C. On the other hand: including left-handers in cognitive neuroscience and neurogenetics. Nat Rev Neurosci. 2014;15(3):193-201.
8.   Kasprian G, Langs G, Brugger PC, Bittner M, Weber M, Arantes M, et al. The Prenatal Origin of Hemispheric Asymmetry: An In Utero Neuroimaging Study. Cerebral Cortex. 2011;21(5):1076-83.
9.   Duboc V, Dufourcq P, Blader P, Roussigne M. Asymmetry of the Brain: Development and Implications. Annual review of genetics. 2015;49:647-72.
10.   Abu-Rustum RS, Ziade MF, Abu-Rustum SE. Reference Values for the Right and Left Fetal Choroid Plexus at 11 to 13 Weeks: An Early Sign of "Developmental" Laterality? Journal of Ultrasound in Medicine. 2013;32(9):1623-9.
11.   Hepper PG, McCartney GR, Shannon EA. Lateralised behaviour in first trimester human foetuses. Neuropsychologia. 1998;36(6):531-4.
12.   Hepper PG, Wells DL, Lynch C. Prenatal thumb sucking is related to postnatal handedness. Neuropsychologia. 2005;43(3):313-5.
13.   Taymourtash A, Schwartz E, Nenning K-H, Sobotka D, Licandro R, Glatter S, et al. Fetal development of functional thalamocortical and cortico–cortical connectivity. Cerebral Cortex. 2022.
14.   Hepper PG. The developmental origins of laterality: Fetal handedness. Developmental Psychobiology. 2013;55(6):588-95.

15.   Francks C. Exploring human brain lateralization with molecular genetics and genomics. Annals of the New York Academy of Sciences. 2015;1359(1):1-13.

16.   Francks C. In search of the biological roots of typical and atypical human brain asymmetry: Comment on "Phenotypes in hemispheric functional segregation? Perspectives and challenges" by Guy Vingerhoets. Phys Life Rev. 2019.

17.   Sha Z, Schijven D, Carrion-Castillo A, Joliot M, Mazoyer B, Fisher SE, et al. The genetic architecture of structural left–right asymmetry of the human brain. Nature Human Behaviour. 2021;5(9):1226-39.

18.   Gunturkun O, Ocklenburg S. Ontogenesis of Lateralization. Neuron. 2017;94(2):249-63.

19.   Medland SE, Duffy DL, Wright MJ, Geffen GM, Hay DA, Levy F, et al. Genetic influences on handedness: Data from 25,732 Australian and Dutch twin families. Neuropsychologia. 2009;47(2):330-7.

20.   de Kovel CGF, Francks C. The molecular genetics of hand preference revisited. Scientific reports. 2019;9(1):5986.

21.   Cuellar-Partida G, Tung JY, Eriksson N, Albrecht E, Aliev F, Andreassen OA, et al. Genome-wide association study identifies 48 common genetic variants associated with handedness. Nature Human Behaviour. 2021;5(1):59-70.

22.   Kong XZ, Mathias SR, Guadalupe T, Group ELW, Glahn DC, Franke B, et al. Mapping cortical brain asymmetry in 17,141 healthy individuals worldwide via the ENIGMA Consortium. Proc Natl Acad Sci U S A. 2018;115(22):E5154-E63.

23.   Guadalupe T, Mathias SR, vanErp TGM, Whelan CD, Zwiers MP, Abe Y, et al. Human subcortical brain asymmetries in 15,847 people worldwide reveal effects of age and sex. Brain imaging and behavior. 2017;11(5):1497-514.

24.   Labache L, Ge T, Yeo BTT, Holmes AJ. Atypical language network lateralization is reflected throughout the macroscale functional organization of cortex. bioRxiv. 2022:2022.12.14.520417.

25.   Somers M, Ophoff RA, Aukes MF, Cantor RM, Boks MP, Dauwan M, et al. Linkage Analysis in a Dutch Population Isolate Shows No Major Gene for Left-Handedness or Atypical Language Lateralization. The Journal of Neuroscience. 2015;35(23):8730-6.

26.   Wiberg A, Ng M, Al Omran Y, Alfaro-Almagro F, McCarthy P, Marchini J, et al. Handedness, language areas and neuropsychiatric diseases: insights from brain imaging and genetics. Brain. 2019.

27.   Sudlow C, Gallacher J, Allen N, Beral V, Burton P, Danesh J, et al. UK biobank: an open access resource for identifying the causes of a wide range of complex diseases of middle and old age. PLoS Med. 2015;12(3):e1001779.

28.   Janke C, Magiera MM. The tubulin code and its role in controlling microtubule properties and functions. Nature Reviews Molecular Cell Biology. 2020;21(6):307-26.

29.   Sha Z, Pepe A, Schijven D, Carrión-Castillo A, Roe JM, Westerhausen R, et al. Handedness and its genetic influences are associated with structural asymmetries of the cerebral cortex in 31,864 individuals. Proceedings of the National Academy of Sciences. 2021;118(47):e2113095118.

30.   McManus IC, Davison A, Armour JAL. Multilocus genetic models of handedness closely resemble single-locus models in explaining family data and are compatible with genome-wide association studies. Annals of the New York Academy of Sciences. 2013:n/a-n/a.

31.   Kavaklioglu T, Ajmal M, Hameed A, Francks C. Whole exome sequencing for handedness in a large and highly consanguineous family. Neuropsychologia. 2016;93:342-9.

32.   Carrion-Castillo A, Van der Haegen L, Tzourio-Mazoyer N, Kavaklioglu T, Badillo S, Chavent M, et al. Genome sequencing for rightward hemispheric language dominance. Genes Brain Behav. 2019;18(5):e12572.

33.   Markou P, Ahtam B, Papadatou-Pastou M. Elevated Levels of Atypical Handedness in Autism: Meta-Analyses. Neuropsychol Rev. 2017;27(3):258-83.

34.   Hirnstein M, Hugdahl K. Excess of non-right-handedness in schizophrenia: meta-analysis of gender effects and potential biases in handedness assessment. Br J Psychiatry. 2014;205(4):260-7.

35.   Postema MC, van Rooij D, Anagnostou E, Arango C, Auzias G, Behrmann M, et al. Altered structural brain asymmetry in autism spectrum disorder in a study of 54 datasets. Nature communications. 2019;10(1):4958-.

36.   Schijven D, Postema MC, Fukunaga M, Matsumoto J, Miura K, de Zwarte SMC, et al. Large-scale analysis of structural brain asymmetries in schizophrenia via the ENIGMA consortium. Proceedings of the National Academy of Sciences. 2023;120(14):e2213880120.

37.   Sha Z, Schijven D, Francks C. Patterns of brain asymmetry associated with polygenic risks for autism and schizophrenia implicate language and executive functions but not brain masculinization. Molecular Psychiatry. 2021;26(12):7652-60.

38.   Satterstrom FK, Kosmicki JA, Wang J, Breen MS, De Rubeis S, An J-Y, et al. Large-Scale Exome Sequencing Study Implicates Both Developmental and Functional Changes in the Neurobiology of Autism. Cell. 2020;180(3):568-84.e23.

39.   Singh T, Poterba T, Curtis D, Akil H, Al Eissa M, Barchas JD, et al. Rare coding variants in ten genes confer substantial risk for schizophrenia. Nature. 2022;604(7906):509-16.

40.   Weiner DJ, Nadig A, Jagadeesh KA, Dey KK, Neale BM, Robinson EB, et al. Polygenic architecture of rare coding variation across 394,783 exomes. Nature. 2023.

41.   Papadatou-Pastou M, Ntolka E, Schmitz J, Martin M, Munafò MR, Ocklenburg S, et al. Human handedness: A meta-analysis. Psychological bulletin. 2020:No Pagination Specified-No Pagination Specified.

42.   Rentzsch P, Witten D, Cooper GM, Shendure J, Kircher M. CADD: predicting the deleteriousness of variants throughout the human genome. Nucleic Acids Research. 2018;47(D1):D886-D94.

43.   Mbatchou J, Barnard L, Backman J, Marcketta A, Kosmicki JA, Ziyatdinov A, et al. Computationally efficient whole-genome regression for quantitative and binary traits. Nat Genet. 2021;53(7):1097-103.

44.   Wu H, Liu Y, Li H, Du C, Li K, Dong S, et al. TRAK1-Mediated Abnormality of Mitochondrial Fission Increases Seizure Susceptibility in Temporal Lobe Epilepsy. Mol Neurobiol. 2021;58(3):1237-47.

45.   Mochizuki Y, Ohashi R, Kawamura T, Iwanari H, Kodama T, Naito M, et al. Phosphatidylinositol 3-Phosphatase Myotubularin-related Protein 6 (MTMR6) Is Regulated by Small GTPase Rab1B in the Early Secretory and Autophagic Pathways*. Journal of Biological Chemistry. 2013;288(2):1009-21.

46.   Amorosi S, D'Armiento M, Calcagno G, Russo I, Adriani M, Christiano A, et al. FOXN1 homozygous mutation associated with anencephaly and severe neural tube defect in human athymic Nude/SCID fetus. Clinical Genetics. 2008;73(4):380-4.

47.   Luscan R, Mechaussier S, Paul A, Tian G, Gérard X, Defoort-Dellhemmes S, et al. Mutations in TUBB4B Cause a Distinctive Sensorineural Disease. The American Journal of Human Genetics. 2017;101(6):1006-12.

48.   Mechaussier S, Dodd DO, Yeyati PL, McPhie F, Attard T, Shoemark A, et al. TUBB4B variants specifically impact ciliary function, causing a ciliopathic spectrum. medRxiv. 2022:2022.10.19.22280748.

49.   Maasz A, Hadzsiev K, Ripszam R, Zsigmond A, Maka E, Knezy K, et al. TUBB4B gene mutation in Leber phenotype of congenital amaurosis syndrome associated with early-onset deafness. European Journal of Medical Genetics. 2022;65(4):104471.

50.   Chen P, Liu Z, Zhang Q, Lin D, Song L, Liu J, et al. DSCAM Deficiency Leads to Premature Spine Maturation and Autism-like Behaviors. The Journal of Neuroscience. 2022;42(4):532-51.

51.   Sollis E, Graham SA, Vino A, Froehlich H, Vreeburg M, Dimitropoulou D, et al. Identification and functional characterization of de novo FOXP1 variants provides novel insights into the etiology of neurodevelopmental disorder. Hum Mol Genet. 2016;25(3):546-57.

52.   Norris DP. Cilia, calcium and the basis of left-right asymmetry. BMC Biol. 2012;10:102.

53.   Fliegauf M, Benzing T, Omran H. When cilia go bad: cilia defects and ciliopathies. Nature reviews Molecular cell biology. 2007;8(11):880-93.

54.   Postema MC, Carrion-Castillo A, Fisher SE, Vingerhoets G, Francks C. The genetics of situs inversus without primary ciliary dyskinesia. Sci Rep. 2020;10(1):3677.

55.   McManus IC, Martin N, Stubbings GF, Chung EM, Mitchison HM. Handedness and situs inversus in primary ciliary dyskinesia. Proc Biol Sci. 2004;271(1557):2579-82.

56.   Vingerhoets G, Li X, Hou L, Bogaert S, Verhelst H, Gerrits R, et al. Brain structural and functional asymmetry in human situs inversus totalis. Brain Struct Funct. 2018.

57.	Tanaka S, Kanzaki R, Yoshibayashi M, Kamiya T, Sugishita M. Dichotic listening in patients with situs inversus: brain asymmetry and situs asymmetry. Neuropsychologia. 1999;37(7):869-74.

58.	Tee YH, Shemesh T, Thiagarajan V, Hariadi RF, Anderson KL, Page C, et al. Cellular chirality arising from the self-organization of the actin cytoskeleton. Nature cell biology. 2015;17(4):445-57.

59.	Fan J, Zhang H, Rahman T, Stanton DN, Wan LQ. Cell organelle-based analysis of cell chirality. Commun Integr Biol. 2019;12(1):78-81.

60.	Inaki M, Liu J, Matsuno K. Cell chirality: its origin and roles in left-right asymmetric development. Philos Trans R Soc Lond B Biol Sci. 2016;371(1710).

61.	Okumura T, Utsuno H, Kuroda J, Gittenberger E, Asami T, Matsuno K. The development and evolution of left-right asymmetry in invertebrates: lessons from Drosophila and snails. Dev Dyn. 2008;237(12):3497-515.

62.	Davison A, McDowell GS, Holden JM, Johnson HF, Koutsovoulos GD, Liu MM, et al. Formin is associated with left-right asymmetry in the pond snail and the frog. Current Biology. 2016;26(5):654-60.

63.	Steinhauer J, Kalderon D. Microtubule polarity and axis formation in the Drosophila oocyte. Dev Dyn. 2006;235(6):1455-68.

64.	McNiven MA, Porter KR. Organization of microtubules in centrosome-free cytoplasm. J Cell Biol. 1988;106(5):1593-605.

65.	Lobikin M, Wang G, Xu J, Hsieh Y-W, Chuang C-F, Lemire JM, et al. Early, nonciliary role for microtubule proteins in left–right patterning is conserved across kingdoms. Proceedings of the National Academy of Sciences. 2012;109(31):12586-91.

66.	McDowell G, Rajadurai S, Levin M. From cytoskeletal dynamics to organ asymmetry: a nonlinear, regulative pathway underlies left-right patterning. Philos Trans R Soc Lond B Biol Sci. 2016;371(1710).

67.	Tischfield MA, Cederquist GY, Gupta ML, Engle EC. Phenotypic spectrum of the tubulin-related disorders and functional implications of disease-causing mutations. Current Opinion in Genetics & Development. 2011;21(3):286-94.

68.	Jaglin XH, Poirier K, Saillour Y, Buhler E, Tian G, Bahi-Buisson N, et al. Mutations in the β-tubulin gene TUBB2B result in asymmetrical polymicrogyria. Nature Genetics. 2009;41(6):746-52.

69.	Shimojima K, Okamoto N, Yamamoto T. A novel TUBB3 mutation in a sporadic patient with asymmetric cortical dysplasia. American Journal of Medical Genetics Part A. 2016;170(4):1076-9.

70.	Fukumura S, Kato M, Kawamura K, Tsuzuki A, Tsutsumi H. A Mutation in the Tubulin-Encoding TUBB3 Gene Causes Complex Cortical Malformations and Unilateral Hypohidrosis. Child neurology open. 2016;3:2329048x16665758.

71.	Baas PW, Lin S. Hooks and comets: The story of microtubule polarity orientation in the neuron. Developmental Neurobiology. 2011;71(6):403-18.

72.	Fu JM, Satterstrom FK, Peng M, Brand H, Collins RL, Dong S, et al. Rare coding variation provides insight into the genetic architecture and phenotypic context of autism. Nat Genet. 2022;54(9):1320-31.

73.	Mitsogiannis MD, Pancho A, Aerts T, Sachse SM, Vanlaer R, Noterdaeme L, et al. Subtle Roles of Down Syndrome Cell Adhesion Molecules in Embryonic Forebrain Development and Neuronal Migration. Frontiers in cell and developmental biology. 2021;8.

74.	Lemieux M, Thiry L, Laflamme OD, Bretzner F. Role of DSCAM in the Development of Neural Control of Movement and Locomotion. International Journal of Molecular Sciences. 2021;22(16):8511.

75.	Braden RO, Amor DJ, Fisher SE, Mei C, Myers CT, Mefford H, et al. Severe speech impairment is a distinguishing feature of FOXP1-related disorder. Developmental Medicine & Child Neurology. 2021;63(12):1417-26.

76.	McManus C. Is any but a tiny fraction of handedness variance likely to be due to the external environment? Laterality. 2021:1-5.

77.	Mitchell KJ. Innate: How the wiring of our brains shapes who we are: Princeton University Press; 2020.

78.	McManus IC. Handedness, language dominance and aphasia: a genetic model. Psychol Med Monogr Suppl. 1985;8:1-40.

79.   Bishop DVM, Bates TC. Heritability of language laterality assessed by functional transcranial Doppler ultrasound: a twin study. 2019;4:161.

80.   Janke C, Bulinski JC. Post-translational regulation of the microtubule cytoskeleton: mechanisms and functions. Nat Rev Mol Cell Biol. 2011;12(12):773-86.

81.   Geiger B, Bershadsky A, Pankov R, Yamada KM. Transmembrane crosstalk between the extracellular matrix--cytoskeleton crosstalk. Nat Rev Mol Cell Biol. 2001;2(11):793-805.

82.   Bycroft C, Freeman C, Petkova D, Band G, Elliott LT, Sharp K, et al. The UK Biobank resource with deep phenotyping and genomic data. Nature. 2018;562(7726):203-9.

83.   Backman JD, Li AH, Marcketta A, Sun D, Mbatchou J, Kessler MD, et al. Exome sequencing and analysis of 454,787 UK Biobank participants. Nature. 2021;599(7886):628-34.

84.   Bycroft C, Freeman C, Petkova D, Band G, Elliott LT, Sharp K, et al. The UK Biobank resource with deep phenotyping and genomic data. Nature. 2018;562(7726):203-9.

85.   Szustakowski JD, Balasubramanian S, Sasson A, Khalid S, Bronson PG, Kvikstad E, et al. Advancing Human Genetics Research and Drug Discovery through Exome Sequencing of the UK Biobank. medRxiv. 2020:2020.11.02.20222232.

86.   Van Hout CV, Tachmazidou I, Backman JD, Hoffman JD, Liu D, Pandey AK, et al. Exome sequencing and characterization of 49,960 individuals in the UK Biobank. Nature. 2020.

87.   Carson AR, Smith EN, Matsui H, Braekkan SK, Jepsen K, Hansen JB, et al. Effective filtering strategies to improve data quality from population-based whole exome sequencing studies. BMC bioinformatics. 2014;15:125.

88.   Cingolani P, Platts A, Wang le L, Coon M, Nguyen T, Wang L, et al. A program for annotating and predicting the effects of single nucleotide polymorphisms, SnpEff: SNPs in the genome of Drosophila melanogaster strain w1118; iso-2; iso-3. Fly. 2012;6(2):80-92.

89.   Liu X, Li C, Mou C, Dong Y, Tu Y. dbNSFP v4: a comprehensive database of transcript-specific functional predictions and annotations for human nonsynonymous and splice-site SNVs. Genome medicine. 2020;12(1):103.

90.   Willer CJ, Li Y, Abecasis GR. METAL: fast and efficient meta-analysis of genomewide association scans. Bioinformatics. 2010;26(17):2190-1.

91.   Coban-Akdemir Z, White JJ, Song X, Jhangiani SN, Fatih JM, Gambin T, et al. Identifying Genes Whose Mutant Transcripts Cause Dominant Disease Traits by Potential Gain-of-Function Alleles. The American Journal of Human Genetics. 2018;103(2):171-87.

92.   Philipp M, Moth CW, Ristic N, Tiemann JKS, Seufert F, Meiler J, et al. MutationExplorer - a webserver for mutation of proteins and 3D visualization of energetic impacts. bioRxiv. 2023:2023.03.23.533926.

93.   Jumper J, Evans R, Pritzel A, Green T, Figurnov M, Ronneberger O, et al. Highly accurate protein structure prediction with AlphaFold. Nature. 2021;596(7873):583-9.